

The X-Ray Astronomy Satellite Astro-C

F. MAKINO *Institute of Space and Astronautical Science 4-6-1 Komaba,
 Meguro-ku, Tokyo, Japan*

THE ASTRO-C TEAM

(Received July 11, 1986)

Astro-C is Japan's third X-ray astronomy satellite, following Hakucho and Tenma, due for launch in February 1987. Main objective of Astro-C is the investigation of time variability of galactic and extragalactic compact X-ray sources in the energy range of 1.5–30 keV. Main instrument is a large-area low-background proportional counter of a 4500 cm² total effective area. The source detection limit will be about 0.1 mCrab. A 0.1 mCrab source can be detected in about 10 min. The highest time resolution for a bright source is 1 msec. In addition, an all sky X-ray monitor and a gamma-ray burst detector are also included.

1. INTRODUCTION

Astro-C is Japan's third and most recent X-ray astronomy satellite scheduled for launch in February 1987. Main objective of Astro-C is a high-sensitivity time variability study of X-ray sources. Both extragalactic and galactic compact X-ray sources exhibit extensive time variabilities in intensity and spectral characteristics on various time scales. Investigations of these time variabilities by previous satellites, including our two X-ray astronomy satellites Hakucho and Tenma, have clearly demonstrated the wealth of information that can be obtained and proven to be extremely important means of increasing our understanding of compact objects and their environments.

Astro-C has a large photo-collection capability by a set of low-background proportional counters with a total effective area of 4500 cm². Among similar instruments launched for the study of time variabilities, the Astro-C experiment will be one of the most sensitive ones to date.

The Astro-C mission is conducted under the responsibility of the Institute of Space and Astronautical Science (ISAS). The experiments of Astro-C are prepared by the groups of ISAS, Nagoya University, Osaka University, Osaka City University, Institute of Cosmic Ray Research, Rikkyo University, University of Leicester (U.K.), Rutherford-Appleton Laboratory (U.K.) and Los Alamos National Laboratory (U.S.A.). This article outlines the scientific objectives of Astro-C followed by general description of the satellite and its experiments.

2. SCIENTIFIC OBJECTS

The large-area proportional counters aboard Astro-C will allow the investigations of time variabilities to be much extended at a substantially higher level of

sensitivity than previous experiments. In this section, we shall briefly discuss the scientific significance of the Astro-C investigations.

(i) *Extragalactic Sources*

Active galactic nuclei (AGN) (i.e., those of radio galaxies, Seyfert galaxies, BL Lacertae type objects and QSO's) display the generation of a huge amount of energy in the form of both electromagnetic radiation as well as matter ejection in cosmic jets. However, the actual mechanism of the central engine responsible for this energy generation is as yet an enigma. X-ray investigations of AGN's are still far from maturity as compared to those of bright galactic sources because of extremely feeble flux from these distant objects. A much higher sensitivity than previously flown instruments is required for detailed study of AGN's.

AGN's are known to exhibit significant X-ray intensity variations on various time scales (Tennant and Mushotzky, 1983). In some cases, drastic intensity changes are found to occur on time scales as short as an hour or even less. Enormous changes in energy output on such short time scales imply that a compact object is involved in the core of the active galaxies and that an efficient release of gravitational energy is taking place through large-scale mass accretion. Since the characteristic time of a large luminosity change must exceed the light travel time across the object, this time gives us an upper limit on the size of the compact nucleus. The small upper limit at present is on the order of 1 A.U., the value obtained for the Seyfert galaxy NGC 6814 (Tennant *et al.* 1981). This upper limit is orders of magnitude smaller than the upper limit thus far obtained from radio observations. Assuming that the observed luminosity from an AGN is near the Eddington limit of the central object, the current upper limit for the size of the central object is already found to be close to the Schwarzschild radius for the mass implied by the luminosity. This has led to the hypothesis that the central compact objects of AGN's are massive black holes. Thus, the importance of refining the current upper limits of active nuclei cannot be overemphasized.

The time scale for large luminosity changes is also related to the efficiency of energy conversion. A large increase in luminosity requires a large increase of accreting mass. This increase in accreting mass results in an increase in the Thomson scattering optical depth which in turn reduces the rate of luminosity increase. Therefore, both the increase in luminosity and its time scale are related to the efficiency of energy conversion. The theoretical limit for the conversion of gravitational energy into radiation is on the order of one tenth the rest mass energy of the accreting matter (one sixth for the case of disk accretion) on a black hole (Fabian and Rees, 1978). On the other hand, there are already cases in which it is suspected that the efficiency of energy conversion exceeds this theoretical limit. Thus, observations of luminosity increases on time scales shorter than previously recorded will lead to implications of fundamental significance.

Investigation of the characteristics and time variation of the energy spectrum of AGN's over a wide energy range is of great value. Changes in spectral shape associated with changes in intensity must be closely related to the energy generation mechanism of AGN's. Also, simultaneous observations at different wavelength bands, radio through UV and X-rays, would greatly enhance our understanding of the AGN structure.

Currently, QSO's are considered to make a significant contribution to the cosmic diffuse X-ray background. Spectral information on QSO's is essential if we are to understand the origin of the diffuse X-ray background. However, available QSO spectra in a wide energy range are as yet very scarce.

(ii) *Galactic Sources*

Periodic and/or aperiodic variations on various time scales are a characteristic feature of galactic compact X-ray sources. Valuable information regarding neutron stars or possibly black holes and their unique environment can be obtained through time variability investigations. Some examples are shown below.

Accurate measurements of the pulse period jitter of X-ray pulsars, which is considered to be due to the response of neutron stars to the fluctuating accretion torque, is an important means to investigate the interior structure of neutron stars (Lamb, 1982).

Rapid and chaotic intensity variations, or flickering, have been observed from several black hole candidates. For instance, flickering on time scales of 1 msec or shorter has been observed from Cyg X-1 (Oda, 1977, Meekins *et al.* 1984). The origin of flickering and its underlying relation to black holes are as yet entirely unknown.

Low-mass binary X-ray sources also exhibit a variety of time variations in intensity and spectrum. Of particular importance is the recent discovery by EXOSAT of the luminosity-dependent quasi-periodic oscillations with periodicities of several tens of msec in the intensities of several low-mass binary X-ray sources (van der Klis *et al.* 1985). The origin of the quasi-periodic oscillations is not satisfactorily explained yet. Besides, it is theoretically expected that neutron stars in low-mass binary sources are rapidly rotating with periods on the order of a few msec. However, any periodic intensity modulation corresponding to such a rapid rotation has not been detected yet. We therefore suspect the rotational modulation to be very small, so that a much higher statistical accuracy than before would be required for the detection.

Many X-ray sources exhibit irregular intensity fluctuations of which the frequency spectrum shows significant "red noise"; increasing power towards lower frequencies (Makishima, 1985). The nature of the red noise is yet to be understood. As regards X-ray bursts, significant and complex time structure in the burst from the Rapid Burster was recently discovered from Tenma (Tawara *et al.* 1985). X-ray bursts from other sources also reveal rapid intensity fluctuations. The particular importance of X-ray bursts is that the phenomenon occurs at the neutron star surface, where significant relativistic effects are expected (Waki *et al.* 1984).

3. GENERAL DESCRIPTION OF ASTRO-C

Astro-C carries the following three experiments:

- (1) Large-area proportional counter (LAC) which is prepared jointly with the

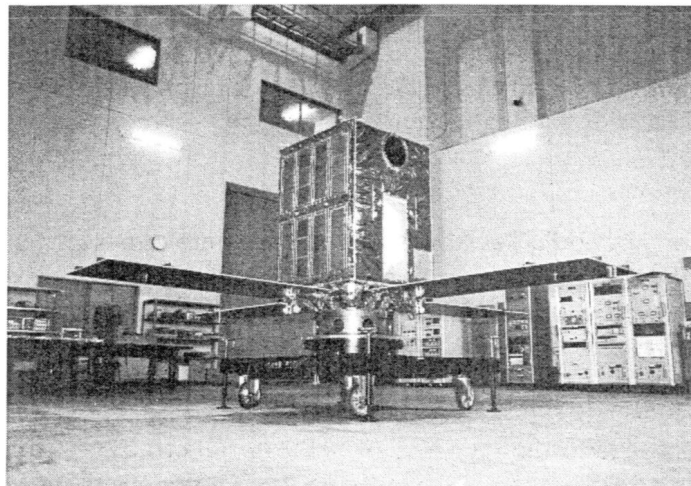


FIGURE 1 The Astro-C satellite. The large-area proportional counter array and one of the two star trackers are visible.

groups of the University of Leicester and Rutherford Appleton Laboratories, the U.K.

(2) All sky X-ray monitor (ASM).

(3) Gamma-ray burst detector (GBD), which is prepared jointly with the group of Los Alamos National Laboratory, U.S.A.

The main characteristics of these experiments will be discussed in sections 3–5.

The Astro-C configuration is shown in Figure 1. The spacecraft weighs approximately 420 kg. The spacecraft is three-axis stabilized by a momentum wheel and a four-gyro inertial reference system. The gyro system is continuously calibrated by two CCD star trackers. The spacecraft maneuvers are carried out with three-axis magnetic torquers. The pointing accuracy will be better than six arcminutes, while the attitude reconstruction will have an accuracy of approximately one arcminute.

The spacecraft Z-axis which is perpendicular to the plane of the solar paddles should be held at angles greater than 135 degrees away from the sun in order to satisfy the power constraints. This constraint limits the observable region of the sky any given time of the year with LAC to within a belt of width ± 45 degrees along a large circle around the sun vector. Except for this seasonal constraint, the entire sky is accessible in a half year.

Data are transmitted downlink at two frequencies, UHF and S-band, with a choice of three different bit rates; 16384 bps (high rate), 2084 bps (medium rate) and 512 bps (low rate). An on-board bubble-memory data recorder with a capacity of 41.9 Mbits can store data for 42 min. 40 sec. at high rate, 5 hr. 41 min. at medium rate and 22 hr. 44 min. at low rate. The stored data will be played back during a ground contact at either 65536 bps (10 min. 40 sec.) or 131072 bps (5 min. 20 sec.).

4. LARGE-AREA PROPORTIONAL COUNTER (LAC).

The large-area proportional counter is the main instrument of Astro-C. It consists of eight multi-cell proportional counters. Figure 2 shows one of these counters. Each counter has an effective area of 565 cm^2 , resulting in a total effective area of 4500 cm^2 .

The field of view is $0.8^\circ \times 1.7^\circ$ with the longer side parallel to the Z-axis, which is defined by honeycomb collimators made of thin stainless steel sheet. A part of the inside surface of the collimators is coated with silver paint in order to eliminate the iron fluorescence line produced in the collimator. The entrance window consists of 63-micron thick beryllium foil, which is supported by the collimators against pressure.

Each counter comprises four layers of anode wires, each anode wire shielded by ground wires. The configuration of the counter wires is shown schematically in Figure 3. The counter is guarded on five sides in order to minimize background counts. All the wires along the counter wall are connected together in two groups (V1, V2) and provide signals for anticoincidence. In addition, anticoincidence pickups (E) are provided on both ends of the counter. The wires in the front layer are grouped into two alternative wires (L1 and R1), whereas the wires in the second and third layers are all connected together (S2-3). Only those events which satisfy exclusive "or" among L1, R1, S2-3 in anticoincidence with V1, V2, E are qualified as X-ray counts. For further background reduction, all counters are shielded with 0.2 mm thick tin. This substantially attenuates the isotropic diffuse background X-ray above 30 keV, which would otherwise be a significant source of background counts.

Counters are filled with a gas mixture of 70% argon, 25% xenon and 5% carbon dioxide at a total pressure of 2 atm. at 20 degree C. The detection efficiency as a function of X-ray energy is shown in Figure 4, for L1 + R1, S2 - 3 and the sum, respectively. The effective energy range in which the detection

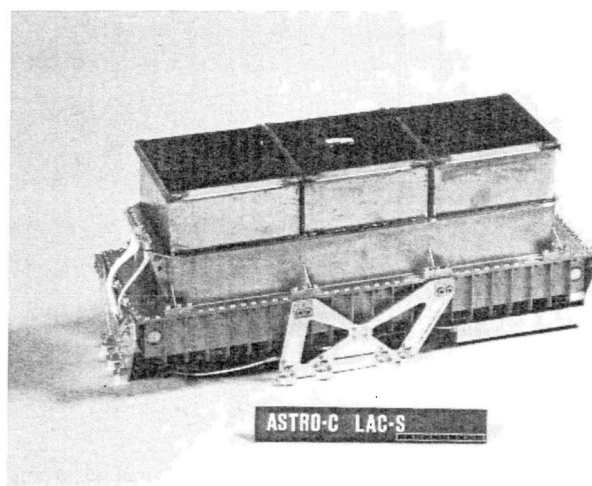


FIGURE 2 One unit of large-area proportional counter. Eight of these are on board.

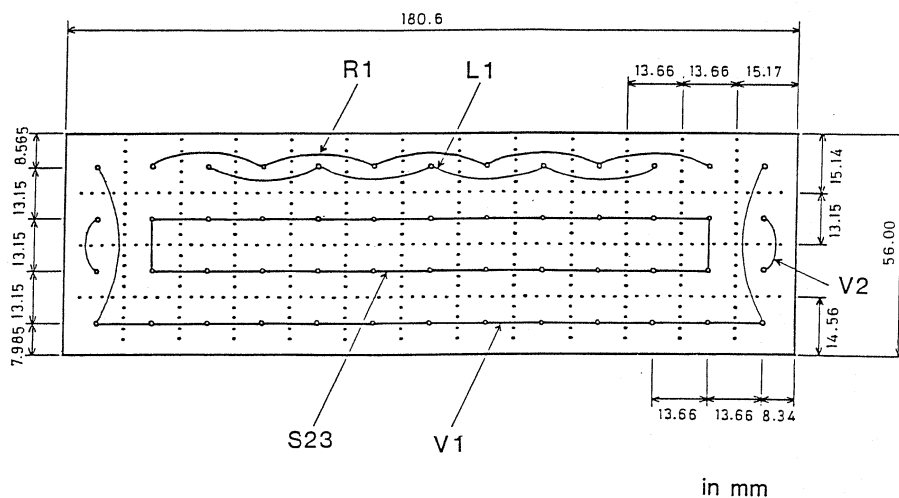


FIGURE 3 Schematic diagram showing the configuration of the counter wires.

efficiency is more than 10% is approximately 1.5 keV to 30 keV. The energy resolution is better than 20% FWHM at 5.9 keV. The in-flight calibration is provided with a ^{109}Cd source (22.1 keV) on each counter which is motor-driven on command.

There are two sources of background counts; the isotropic diffuse X-ray

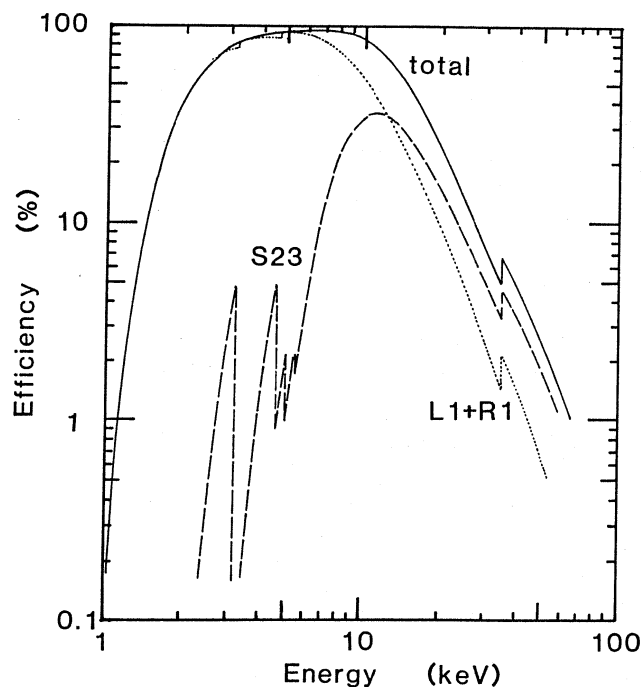


FIGURE 4 Detection efficiency of the proportional counters as a function of energy. The dashed, dotted, and solid curves represent the efficiencies for S2-3, L1+R1, and their sum, respectively. Reduction of efficiency for X-ray above the Xe K-edge by the anti-coincidence is taken into account.

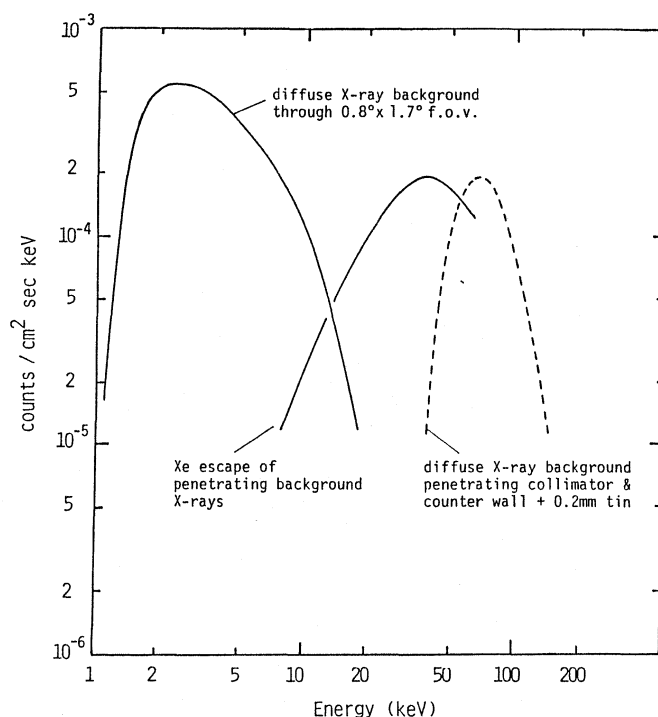


FIGURE 5 Expected background spectrum due to the diffuse X-ray background.

background and cosmic-ray induced background. The expected background spectrum due to the diffuse X-ray background is shown in Figure 5. This consists of two parts; (i) direct flux incident through the collimator field of view and (ii) high energy X-rays penetrating the counter wall or collimator. The total background count rate in orbit summed over all eight counters is estimated to be 12 counts/sec from isotropic diffuse background and roughly 30 counts/sec from cosmic-ray induced background. The count rate of vetoed events is recorded in order to monitor the variation of the cosmic-ray induced background.

Qualified X-ray events are pulse-height analysed into a maximum of 48 channels. There are four modes of observation as listed in Table I. Time

TABLE I
Observational modes vs. time resolution

Mode	No. of Pulse Height Ch.	High	Bit Rate Medium	Low	No. of Output Signals
1	48	0.5 s	4.0 s	16.0 s	8, each of 8 counters
2	48	62.5 ms	0.5 s	2.0 s	2, sums of 4 counters
3	12	7.8 ms	62.5 ms	0.25 s	1, sum of all 8 counters
4	2	H 1.9 ms L 0.98 ms	15.6 ms 7.8 ms	62.5 ms 31.3 ms	2, sums of 4 counters

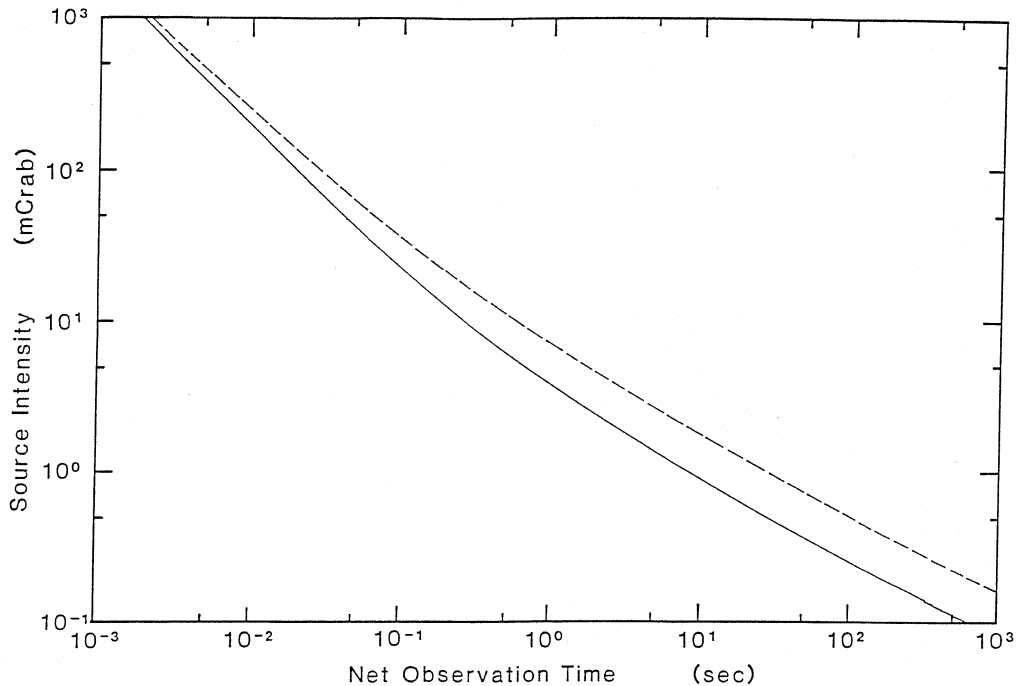


FIGURE 6 Sensitivity of the LAC experiment. The observation time to detect a source at a 5σ confidence is shown as a function of the source intensity. The time indicated by the dashed curve includes both on- and off-source observations, whose ratio is optimized for minimizing the statistical error. The solid curve represents the case in which the background rate is known and no off-source observation is performed.

resolution is mode-dependent. The highest time resolution available is 0.98 msec at the expense of spectral information. A suitable mode will be chosen depending on the objective, in consideration of counting rate, time resolution and length of recording, etc.

The sensitivity required for detection of sources and the measurement of intensity variations is of scientific interest. Figure 6 illustrates the time required for the detection of a source at the 5σ level as a function of source intensity. The detection limit depends on the knowledge of the background count rate and on its stability. Our experience has shown that the safe detection limit is on the order of 5% of the background rate, provided that the cosmic ray intensity is separately monitored as stable. We expect a detection limit of approximately 0.1 mCrab intensity, or 2×10^{-12} ergs/cm²sec in the range 2–10 keV. The source detection at this intensity level can be achieved in about 10 minutes. In addition, on- and off-source switching will enhance the source detection capability. For the present $0.8^\circ \times 1.7^\circ$ field of view, this detection limit is close to the limit imposed by source confusion.

The sensitivity required to detect intensity variations is shown in Figure 7 for two cases; a weak source of 1 mCrab intensity and an intense source of 1 Crab intensity. In the case of a source of 1 mCrab intensity, typical of extragalactic sources, an intensity increase or decrease of 50% is detected with 5σ confidence

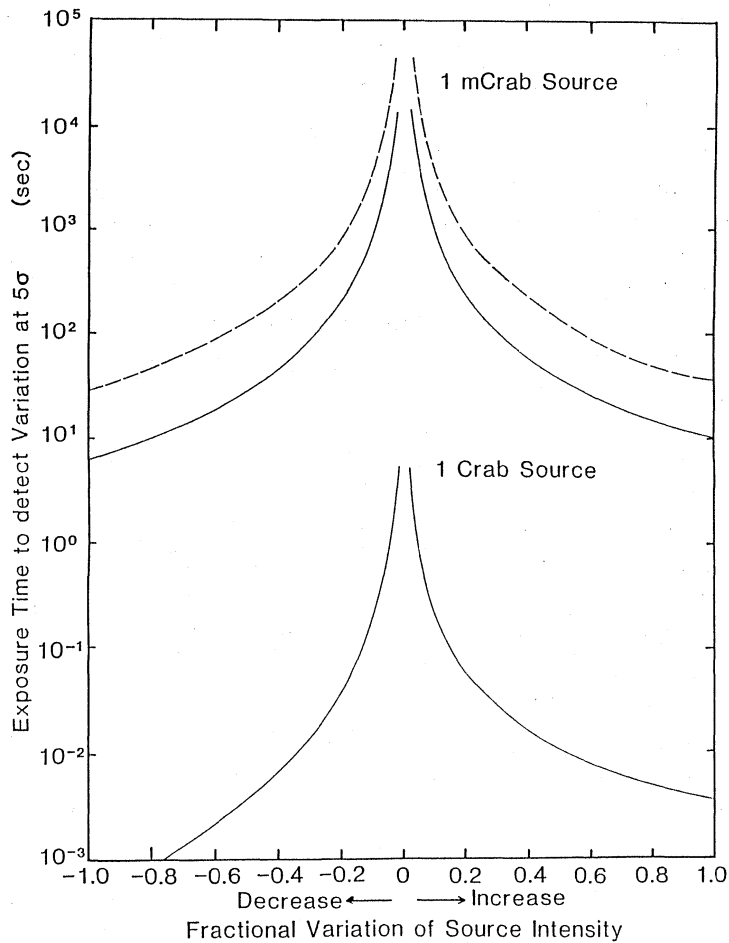


FIGURE 7 Sensitivity of detecting source intensity changes. The exposure time required to detect an intensity change at a 5σ confidence is shown for a 1 mCrab source and a 1 Crab source, respectively. The amount of intensity change is expressed in terms of the fraction of the pre-increase or pre-decrease level. The dashed and solid curves are with and without inclusion of the optimum observation time before the change, respectively.

in about 50 sec. On the other hand, in the case of an intense source of 1 Crab intensity, an intensity increase by 50% is detectable in about 20 msec and a 50% decrease (drop to one half) can be detected in less than 2 msec, both at 5σ confidence level. These figures demonstrate the significance of Astro-C observations of time variations in both AGN's and bright galactic X-ray sources.

5. ALL SKY MONITOR (ASM)

This experiment continuously monitors many sources in a wide area of the sky and records significant intensity variations as well as transient phenomena. ASM consists of two proportional counters, each having three independent counting cells and field of view criss-cross to each other. The effective area of each cell is

67 cm², resulting in a total effective area of 400 cm². The counters are filled with 1 atm. of Xe, and the windows are 50 microns-thick beryllium. The effective energy range is approximately 1.5–30 keV.

The field of view of each cell is defined by a stacked-mesh collimator to $1^\circ \times 45^\circ$ FWHM, and is tilted with respect to the spacecraft Z-axis. Different slant angles for the individual cells will resolve source confusion. A scan of the sky is performed by slowly rotating the spacecraft around the Z-axis at a fixed slew rate of 20 min/revolution or 0.3°/sec. A source of 40 mCrab intensity will be detected at the 3σ significance level in a single scan. The source position can be determined with an accuracy of better than $1^\circ \times 1^\circ$. Scan of the sky will be performed during the time of earth occultation of the target object and in between successive observations.

6. GAMMA-RAY BURST DETECTOR (GBD)

This experiment is designed to detect gamma-ray bursts with a high time resolution and measure the burst spectra over a substantially wider energy range than has been previously covered. The instrument consists of a proportional counter (PC) and a NaI(Tl) scintillation counter (SC). Figure 8 shows the efficiency versus energy for the two different detectors together.

The proportional counter has a 100 cm² effective area with 64 micron-thick beryllium window and is filled with 1 atm. of Xe. No collimator is installed. The proportional counter covers the energy range of approximately 1.5–30 keV. Each event is pulse-height analysed in 16 channels on a pseudo-logarithmic scale.

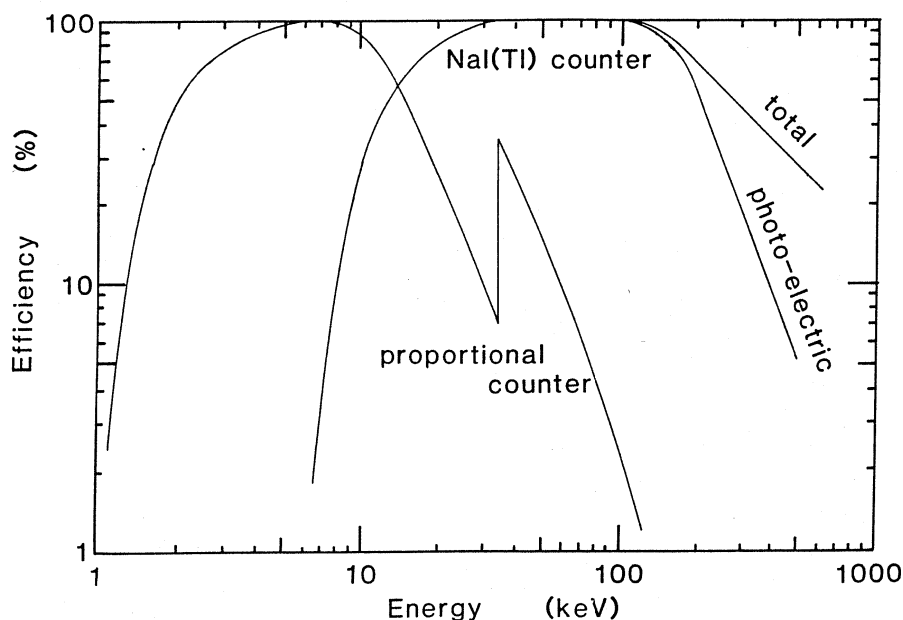


FIGURE 8 Detection efficiency of the GBD counters as a function of energy for the case of normal incidence. The geometrical factor becomes maximum at about 45° .

The NaI(Tl) scintillator has an effective area of 60 cm^2 and a thickness of 1 cm, with a 0.25 mm-thick aluminum window. Again, no collimator is installed. The scintillation counter detects hard X-rays in the energy range of approximately 10–400 keV. Each event is pulse-height analysed in 32 channels on a pseudo logarithmic scale. The counter is in-flight calibrated with a 59.5 keV line from a weak ^{241}Am source flagged by coincidence with α -particle detection by a small solid state detector on which the source is mounted.

A separate solid state detector of 1 cm^2 area monitors the radiation environment and produces a warning signal whenever an excessive flux is recorded, such as is the case upon entering the radiation belt. This signal is also distributed to LAC and ASM.

A gamma-ray burst is registered by a sudden increase of count rate in either of PC and SC or both. A burst-flag generator is triggered when the increment of counts within a present time interval (one of 1/4, 1.4 sec) exceeds n ($n = 8$ or 11) of the average rate for the last 16 sec. If that occurs, data for PC(SC) over the period between 32(16) sec before and 96(48) sec after the burst flag onset are stored in a 14 kbyte temporary memory and are read out during the next play-back. This enables us to recover the whole burst profile. Data contain the flag onset time to an accuracy of 244 microsec and a train of counts in every 31.25 msec. Time-to-spill mode is provided to prevent scaler overflow. Pulse height analysis is performed at the same time in every 1/2 sec.

Minimum detectable burst size is estimated to be roughly $3 \times 10^{-6} \text{ ergs/cm}^2\text{sec}$. Hopefully, this experiment will provide us with spectrum of gamma-ray bursts and its time evolution is a very wide energy range, in particular in soft X-rays where previous data are scarce.

REFERENCES

- Tennant, A. F., and Mushotzky, R. F., 1983, *Astrophys. J.*, **264**, 92.
 Tennant, A. F. *et al.*, 1981, *Astrophys. J.* **251**, 15.
 Fabian, A. C., and Rees, M. J., 1978, in *X-ray Astronomy*, ed. W. A. Baity and L. E. Peterson, Proc. of COSPAR Symposium, *Adv. in Space Expl.* **3**, 381.
 Lamb, F. K., 1982, in *Accreting Neutron Stars*, ed. W. Brinkmann and J. Trumper, p. 316, MPE.
 Oda, M., 1977, *Space Sci. Rev.* **20**, 757. Meekins, J. F., *et al.*, 1984, *Astrophys. J.* **278**, 288.
 van der Klis, M. *et al.*, 1985, *Nature* **316**, 225.
 Makishima, K., 1985, in *Workshop on the Timing Studies of X-ray Sources*, ed. S. Hayakawa and F. Nagase, p. 65.
 Tawara, Y. *et al.*, 1985, *Nature* **318**, 545.
 Waki, I. *et al.*, 1984, *Publ. Astron. Soc. Japan* **36**, 819.